

# Using the $e^\pm\mu^\mp + E_T^{miss}$ and $l^+l^- + E_T^{miss}$ Signatures in the Search for Supersymmetry and Constraining the MSSM model at LHC

Yu.Andreev, N.Krasnikov and A.Toropin  
Institute for Nuclear Research RAS, Moscow, 117312, Russia

November 8, 2018

## Abstract

We study the  $e^\pm\mu^\mp + E_T^{miss}$  and  $l^+l^- + E_T^{miss}$  signatures ( $l = e, \mu$ ) for different values of  $\tan\beta$  in the mSUGRA model. With  $\tan\beta$  rising, we observe a characteristic change in the shape of dilepton mass spectra in  $l^+l^- + E_T^{miss}$  versus  $e^\pm\mu^\mp$  final states reflecting the decrease of  $\tilde{\chi}_2^0 \rightarrow l^+l^- \tilde{\chi}_1^0$  branching ratio. We also study the non mSUGRA modifications of the CMS test point LM1 with arbitrary relations among gaugino and higgsino masses. For such modifications of the mSUGRA test point LM1 the number of lepton events depends rather strongly on the relations among gaugino and higgsino masses and in some modifications of the test point LM1 the signatures with leptons and  $E_T^{miss}$  do not lead to the SUSY discovery and the single SUSY discovery signature remains the signature with  $n \geq 2$  *jets* +  $E_T^{miss}$  + *no leptons*.

# 1 Introduction

One of the goals of the Large Hadron Collider (LHC) [1] is the discovery of supersymmetry (SUSY). The squark and gluino decays produce missing transverse energy  $E_T^{miss}$  from lightest stable superparticle (LSP) plus multiple jets and isolated leptons [1]. One of the most interesting and widely discussed signatures for SUSY discovery at the LHC is the signature with two opposite charge and the same flavour leptons [2]:  $l^+l^- + E_T^{miss}$ . The main reason of such interest is that neutralino decays into leptons and LSP  $\tilde{\chi}_2^0 \rightarrow l^+l^-\tilde{\chi}_1^0$  contribute to this signature and the distribution of the  $l^+l^-$  invariant mass  $m_{inv}(l^+l^-)$  has the edge structure [3] that allows to determine some combination of the SUSY masses.

The signature  $e^\pm\mu^\mp + E_T^{miss}$  can be realized when  $\chi_2^0$  decays into  $\tau$  pair which is only relevant at large  $\tan\beta$  [4]. Also as it is shown in Ref.[3] at the level of CMSJET [5] simulation the use of  $e^\pm\mu^\mp + E_T^{miss}$  signature for large  $\tan\beta$  allows to obtain nontrivial information on parameters of the decay  $\tilde{\chi}_2^0 \rightarrow \tilde{\tau}\tau \rightarrow \tau\tau\tilde{\chi}_1^0 \rightarrow e^\pm\mu^\mp\tilde{\chi}_1^0\nu\nu\bar{\nu}\bar{\nu}$ . On the other hand, the  $e^\pm\mu^\mp + E_T^{miss}$  (with an arbitrary number of jets) can be used for the detection of lepton flavour violation in slepton decays [6], [7] at the LHC.

In the Minimal Supersymmetric Model (MSSM) [8] supersymmetry is broken at some high scale  $M$  by generic soft terms, so in general all soft SUSY breaking terms are arbitrary which complicates the analysis and spoils the predictive power of the theory. In the Minimal Supergravity Model (mSUGRA) [8] the universality of the different soft parameters at the Grand Unified Theory (GUT) scale  $M_{GUT} \approx 2 \cdot 10^{16}$  GeV is postulated. Namely, all the spin zero particle masses (squarks, sleptons, higgses) are postulated to be equal to the universal value  $m_0$  at the GUT scale. All gaugino particle masses are postulated to be equal to the universal value  $m_{1/2}$  at GUT scale. Also the coefficients in front of quadratic and cubic SUSY soft breaking terms are postulated to be equal. The renormalization group equations are used to relate GUT and electroweak scales. The equations for the determination of a nontrivial minimum of the electroweak potential are used to decrease the number of the unknown parameters by two. So the mSUGRA model depends on five unknown parameters. At present, the more or less standard choice of free parameters in the mSUGRA model includes  $m_0, m_{1/2}, \tan\beta, A$  and  $sign(\mu)$  [8]. All sparticle masses depend on these parameters.

In Ref.[9] the possibility to detect SUSY and lepton flavour violation using the  $e^\pm\mu^\mp + E_T^{miss}$  signature at the LHC for the Compact Muon Solenoid

(CMS) detector at the level of full detector simulation was studied. Note also Ref.[10] where the SUSY mSUGRA CMS detector discovery potential was investigated for the  $l^+l^- + E_T^{miss}$  signature at the level of full detector simulation.

In this paper we study the  $e^\pm\mu^\mp + E_T^{miss}$  and  $l^+l^- + E_T^{miss}$  signatures ( $l = e, \mu$ ) for different values of  $\tan\beta$  in the mSUGRA model. With  $\tan\beta$  rising, we observe a characteristic change in the shape of dilepton mass spectra in  $l^+l^- + E_T^{miss}$  versus  $e^\pm\mu^\mp$  final states reflecting the decrease of  $\tilde{\chi}_2^0 \rightarrow l^+l^- \tilde{\chi}_1^0$  branching ratio. We also study the non mSUGRA modifications of the CMS test point LM1 with arbitrary relations among gaugino and higgsino masses. For such modifications of the mSUGRA test point the number of lepton events depends rather strongly on the relations among gaugino and higgsino masses and in some modifications of test point LM1 the signatures with leptons and  $E_T^{miss}$  do not lead to the SUSY discovery and the single SUSY discovery signature remains the signature with  $n \geq 2$  jets +  $E_T^{miss}$  + no leptons.

The organization of the paper is the following. Section 2 describes some useful technical details of performed simulations. In Section 3 the backgrounds and cuts used to suppress the backgrounds are discussed. Section 4 contains the results of numerical calculations concerning the possibility to detect SUSY and constrain the SUSY parameters using the  $e^\pm\mu^\mp + E_T^{miss}$  and  $l^+l^- + E_T^{miss}$  signatures. Section 5 contains the results of the simulations for different values of  $\tan\beta$ . In Section 6 we discuss the results of the simulation of the MSSM with nonuniversal gaugino and higgsino masses. Section 7 contains concluding remarks.

## 2 Simulation details

The coupling constants and cross sections in the leading order (LO) approximation for SUSY processes and backgrounds were calculated with ISASUGRA 7.69 [11], PYTHIA 6.227 [12] and CompHEP 4.2pl [13]. For the calculation of the next-to-leading order (NLO) corrections to the SUSY cross sections the PROSPINO [14] code was used. For considered signal events and backgrounds the NLO corrections are known and the values of NLO cross sections (or  $k$ -factors) were used for normalization of the numerical results. We used the full simulation results of Ref.[9] for the estimation of the number of background events. The CMS fast simulation code *FAMOS\_1.4.0* [15] was used for the estimation of signal events.

The reconstructed electrons and muons were passed through packages defining lepton isolation criteria. For each electron and muon the following parameters were defined:

- *TrackIsolation* is a number of additional tracks with  $p_T > 2 \text{ GeV}/c$  inside a cone with  $R \equiv \sqrt{\Delta\eta^2 + \Delta\Phi^2} < 0.3$  around the lepton.
- *CaloIsolation* is a ratio of energy deposited in the calorimeters (electromagnetic (ECAL) + hadronic (HCAL)) inside a cone with  $R = 0.13$  around given track to the energy deposited inside a cone with  $R = 0.3$ .
- *HERatio* is defined as a ratio of energy deposited in the HCAL inside a cone with  $R = 0.13$  to the energy deposited in the ECAL inside the same cone.
- *EPratio* is a ratio of energy deposited in the ECAL inside a cone with  $R = 0.13$  to the momentum of the reconstructed track.

### 3 Signal selection and backgrounds

The SUSY production  $pp \rightarrow \tilde{q}\tilde{q}', \tilde{g}\tilde{g}, \tilde{q}\tilde{g}$  with subsequent decays

$$\tilde{q} \rightarrow q' \tilde{\chi}_{1,2}^\pm, \quad (1)$$

$$\tilde{g} \rightarrow q\tilde{q}' \tilde{\chi}_{1,2}^\pm, \quad (2)$$

$$\tilde{\chi}_{1,2}^+ \rightarrow \tilde{\chi}_1^0 e^+ (\mu^-) \nu, \quad (3)$$

$$\tilde{\chi}_{1,2}^- \rightarrow \tilde{\chi}_1^0 \mu^- (e^-) \nu, \quad (4)$$

lead to the event topologies  $e^\pm \mu^\mp + E_T^{miss}$  and  $l^+ l^- + E_T^{miss}$ . Note that in the MSSM with lepton flavour conservation neutralino decays into leptons  $\tilde{\chi}_{2,3,4}^0 \rightarrow l^+ l^- \tilde{\chi}_1^0$  ( $l \equiv e, \mu$ ) do not contribute into the  $e^\pm \mu^\mp + E_T^{miss}$  signature. The main backgrounds which contribute to the  $e^\pm \mu^\mp$  events are:  $t\bar{t}$ , WW, WZ, ZZ, Wt, Zbb,  $\tau\bar{\tau}$  and Z+jet. It is found that  $t\bar{t}$  is the largest background and it gives more than 50% contribution to the total background. In this paper we used the results of Ref.[9] for the estimation of the number of background events.

In the analysis the events with the following isolation criteria for electrons were used: *TrackIsolation* < 1.0, *CaloIsolation* > 0.85,  $0.85 <$

$EPratio < 2.0$ ,  $HEratio < 0.25$ . The same criteria for muons were the following:  $TrackIsolation < 1.0$ ,  $CaloIsolation > 0.50$ ,  $EPratio < 0.20$ ,  $HEratio > 0.70$ . These numbers were adjusted by studying electron and muon tracks in the process  $pp \rightarrow WW \rightarrow 2l$ .

The selection cuts are the following:

- cut on leptons:  $p_T^{lept} > p_T^{lept,0}$ ,  $|\eta| < 2.4$ , lepton isolation within  $\Delta R < 0.3$  cone
- cut on missing transverse energy:  $E_T^{miss} > E_T^{miss,0}$ .

Here  $p_T^{lept,0}$  and  $E_T^{miss,0}$  are corresponding thresholds.

## 4 Use of the $e^\pm\mu^\mp + E_T^{miss}$ signature for the SUSY detection

In this section we remind the main results of Ref.[9] on SUSY detection using the  $e^\pm\mu^\mp + E_T^{miss}$  signature. The possibility to detect SUSY using the CMS test points LM1 - LM9 [16] chosen for the detailed study of SUSY detection at the CMS was investigated in Ref.[9]. This study was based on the counting the expected number of events for both the Standard Model (SM) and the mSUGRA model. The parameters of the CMS test points LM1 - LM9 are given in Table 1.

Table 1: The parameters of the CMS test points.

Point	$m_0$ (GeV)	$m_{1/2}$ (GeV)	$\tan\beta$	$sign(\mu)$	$A_0$
LM1	60	250	10	+	0
LM2	185	350	35	+	0
LM3	330	240	20	+	0
LM4	210	285	10	+	0
LM5	230	360	10	+	0
LM6	85	400	10	+	0
LM7	3000	230	10	+	0
LM8	500	300	10	+	-300
LM9	1450	175	50	+	0

For the point LM1 (the point LM1 coincides with the post-WMAP point B [17]) it was found that the cuts with  $p_T^{lept} > 20 \text{ GeV}/c$ ,  $E_T^{miss} > 300 \text{ GeV}$  are close to the optimal ones (the highest significance with the best signal/background ratio). The results for the luminosity  $\mathcal{L} = 10 \text{ fb}^{-1}$  are presented in Table 2. For other CMS SUSY test points LM2 - LM9 the results with the same cuts are presented in Table 3. The significances in this table are the following:  $S_{c12} = 2(\sqrt{N_S + N_B} - \sqrt{N_B})$  [18] and  $S_{cL} = \sqrt{2((N_S + N_B) \ln(1 + N_S/N_B) - N_S)}$  [19].

Table 2: The expected number of events for backgrounds and for signal at the point LM1,  $\mathcal{L} = 10 \text{ fb}^{-1}$ ,  $e^\pm \mu^\mp + E_T^{miss}$  signature.

Process	2 isolated leptons, $p_T^{lept} > 20 \text{ GeV}/c$	$E_T^{miss} > 300 \text{ GeV}$
t $\bar{t}$	39679	79
WW	4356	4
WZ	334	2
ZZ	38	0
Wt	3823	2
Zbb	315	0
Z+jet	1082	6
DY2 $\tau$	7564	0
SM background	57191	93
LM1 Signal	1054	329

It was found from the Tables 2-3 that for the point LM1 the significances are  $S_{c12} = 21.8$  and  $S_{cL} = 24.9$  for the  $e^\pm \mu^\mp + E_T^{miss}$  signature.

The supersymmetry discovery potential for the mSUGRA model with  $\tan\beta = 10$ ,  $sign(\mu) = +$  in the  $(m_0, m_{1/2})$  plane (generalization of the point LM1) using the CMS fast simulation program *FAMOS\_1.4.0* [15] was also studied. The CMS discovery potential contours for  $\mathcal{L} = 1, 10$  and  $30 \text{ fb}^{-1}$  for the signature  $e^\pm \mu^\mp + E_T^{miss}$  are shown in Fig.1.

Table 3: The number of signal events and significances for the cuts with  $p_T^{lept} > 20$  GeV/ $c$  and  $E_T^{miss} > 300$  GeV for  $\mathcal{L} = 10$  fb $^{-1}$ , signature  $e^\pm \mu^\mp + E_T^{miss}$ . The number of the SM background events  $N_B = 93$  (see Table 2).

Point	$N$ events	$S_{c12}$	$S_{cL}$
LM1	329	21.8	24.9
LM2	94	8.1	8.6
LM3	402	25.2	29.2
LM4	301	20.4	23.1
LM5	91	7.8	8.3
LM6	222	16.2	18.0
LM7	14	1.4	1.4
LM8	234	16.9	18.8
LM9	137	11.0	11.9

## 5 The shape of the dilepton mass distribution in the mSUGRA parameter space

At the LHC neutralinos  $\tilde{\chi}_2^0$  are dominantly produced in the decay chain of gluino and squarks, for instance  $\tilde{g} \rightarrow q\bar{q}\tilde{\chi}_2^0$  or  $\tilde{q} \rightarrow q\tilde{\chi}_2^0$  and  $\tilde{\chi}_j^0 \rightarrow \tilde{\chi}_2^0 Z^0$ . Within the mSUGRA model in the domain of relatively small  $m_0$  ( $m_0 \leq 0.6m_{1/2}$ ) the following leptonic decays of  $\tilde{\chi}_2^0$  are the most important:

$$\tilde{\chi}_2^0 \rightarrow \tilde{\chi}_1^0 l^+ l^-, \quad (5)$$

$$\tilde{\chi}_2^0 \rightarrow \tilde{l}_L l, \quad (6)$$

$$\tilde{\chi}_2^0 \rightarrow \tilde{l}_R l, \quad (7)$$

$$\tilde{\chi}_2^0 \rightarrow \tilde{\tau}_1 \tau, \quad (8)$$

$$\tilde{\chi}_2^0 \rightarrow \tilde{\chi}_1^0 \tilde{\tau}_1 \tau_1. \quad (9)$$

In mSUGRA for the case when  $\tilde{\chi}_2^0$  decays into lepton and slepton are kinematically allowed, the sleptons decay directly into LSP with  $Br(\tilde{l}_{L,R} \rightarrow l\tilde{\chi}_1^0) \sim 1$  and  $Br(\tilde{\tau}_1 \rightarrow \tau\tilde{\chi}_1^0) \sim 1$ . With the increase of  $\tan\beta$  the  $\tilde{\tau}_1$  mass is decreased and as a consequence the branching ratio  $Br(\tilde{\chi}_2^0 \rightarrow \tilde{\tau}_1 \tau)$  is increased whereas the branching ratio  $Br(\tilde{\chi}_2^0 \rightarrow \tilde{l}_{R,L} l)$  is decreased, see Fig.2.

The process  $\tilde{\chi}_2^0 \rightarrow \tilde{l}l \rightarrow ll\tilde{\chi}_1^0$  has the edge structure for the distribution of lepton-pair invariant mass  $m_{ll}$  and the edge mass  $m_{inv}^{max}(l^+l^-)$  is expressed by slepton mass  $m_{\tilde{l}}$  and neutralino masses  $m_{\tilde{\chi}_{1,2}^0}$  as follows [3]:

$$(m_{inv}^{max}(l^+l^-))^2 = m_{\tilde{\chi}_2^0}^2 \left(1 - \frac{m_{\tilde{l}}^2}{m_{\tilde{\chi}_2^0}^2}\right) \left(1 - \frac{m_{\tilde{\chi}_1^0}^2}{m_{\tilde{l}}^2}\right) \quad (10)$$

The corresponding  $m_{inv}^{max}(\tau^+\tau^-)$  edge maximum due to  $\tilde{\chi}_2^0$  decays to stau's has a maximum at:

$$(m_{inv}^{max}(\tau^+\tau^-))^2 = m_{\tilde{\chi}_2^0}^2 \left(1 - \frac{m_{\tilde{\tau}_1}^2}{m_{\tilde{\chi}_2^0}^2}\right) \left(1 - \frac{m_{\tilde{\chi}_1^0}^2}{m_{\tilde{\tau}_1}^2}\right) \quad (11)$$

But the spectrum of the dilepton same flavour opposite sign channel proceeding through  $\tau \rightarrow l\nu\bar{\nu}$  decays is not so pronounced as the spectrum from  $\tilde{\chi}_2^0 \rightarrow \tilde{l}l \rightarrow ll\tilde{\chi}_1^0$  decay due to the missing momentum taken by four neutrinos from  $\tau$  decays. In particular the  $l^+l^-$  invariant mass is distributed in the lower mass region below the expected ditau kinematical point. Thus, a distinctive feature of the  $m_{inv}(l^+l'^-)$  spectrum from  $\tilde{\chi}_2^0$  decays to staus is distributed in the lower mass region below the expected ditau kinematical end point. With increase of  $\tan\beta$ , due to significant increase of  $\tilde{\chi}_2^0$  decays into stau's and the corresponding decrease of decays into selectrons and smuons, a deterioration of the sharpeness of the  $l^+l^-$  dilepton edge takes place [4]. Another consequence of the change in the relative branching ratios of these decays is that the event rate difference between  $e^+e^- + \mu^+\mu^-$  and  $e^+\mu^- + \mu^+e^-$  channels decreases [4]. To illustrate the behaviour of the  $m_{inv}(l^+l^-)$  and  $m_{inv}(l^+l'^-)$  spectra at different  $\tan\beta$  we investigated several mSUGRA points, namely:

- a. The generalization of the point LM1 ( $m_0 = 60 \text{ GeV}, m_{1/2} = 250 \text{ GeV}, A = 0, \text{sign}(\mu) = +, \tan\beta = 10$ ) with  $\tan\beta = 15, 20, 25, 30, 35$ .
- b. The points with  $m_0 = 100 \text{ GeV}, m_{1/2} = 300 \text{ GeV}, A = 300 \text{ GeV}, \text{sign}(\mu) = +$  and  $\tan\beta = 10, 15, 20, 25, 30, 35$ .
- c. The points with  $m_0 = 300 \text{ GeV}, m_{1/2} = 300 \text{ GeV}, A = 0, \text{sign}(\mu) = +$  and  $\tan\beta = 10, 15, 20, 25, 30, 35$ .
- d. The points with  $m_0 = 2500 \text{ GeV}, m_{1/2} = 250 \text{ GeV}, A = 0, \text{sign}(\mu) = +$  and  $\tan\beta = 10, 15, 20, 25, 30, 35$ .

For the points (a) and (b) sleptons are lighter than  $\tilde{\chi}_2^0$  that leads to the existence of well-defined edge structure in the  $m_{inv}(l^+l^-)$  structure for not very large values of  $\tan\beta$ . For the points (c) and (d) the sleptons are heavier



than  $\tilde{\chi}_2^0$  and the dominant decay mode is  $\tilde{\chi}_2^0 \rightarrow Z + \tilde{\chi}_1^0$  with the branching ratio close to 100%.

For these mSUGRA points we have made calculations using FAMOS fast simulation program for the integrated luminosity  $\mathcal{L} = 1 \text{ fb}^{-1}$ . The results of our simulations are presented in Figs.2 - 7.

As one can see from Figs.2 - 7 with  $\tan \beta$  rising there is a characteristic change in the shape of dilepton  $l^+l^-$  mass spectra versus  $e^\pm\mu^\mp$  mass spectra resulting in the increase of the ratio of  $N_S(l^+l^-)/N_S(e^\pm\mu^\mp)$  signal events. As it has been mentioned before this behaviour is due to the increase of  $Br(\tilde{\chi}_2^0 \rightarrow \tilde{\tau}\tau)$  and decrease of  $Br(\tilde{\chi}_2^0 \rightarrow \tilde{l}l)$  with the rising of  $\tan \beta$ .

## 6 The dileptons for the case of nonuniversal gaugino masses

In this section we present the results of our simulations for the case of nonuniversal gaugino masses. Namely, we consider the deformations of the test point LM1 violating gaugino mass universality assumption, see Table 4.

Table 4: Values of factors for masses increasing (unity if not indicated) in comparison with the masses of the point LM1.

Point	$M_1$	$M_2$	$M_3$	$\mu$	$m_2$	$m_{\tilde{q}}$
1		2				
2		4				
3		8				
4		2		2		
5		4		4		
6		8		8		
7	2	4	5	4		
8	3	4	5	4		
9	2	4	5	4	5	
10	3	4	5	4	5	
11						10
12	2	2				10

In Table 4  $M_1$ ,  $M_2$  and  $M_3$  are  $U(1)$ ,  $SU(2)$  and  $SU(3)$  gaugino masses

correspondingly and  $\mu$  is higgsino mass parameter.  $m_2$  means masses of the first two squark and slepton generations and  $m_{\tilde{q}}$  means all squark and slepton masses.

Points (1 - 3) differ from CMS mSUGRA test point LM1 by  $SU(2)$  gaugino mass  $M_2$ . The dependence of  $m_{inv}(l^+l^-)$  and  $m_{inv}(e^\pm\mu^\mp)$  invariant spectra for the point LM1 and the points (1 - 3) are shown in Fig.8. With the increase of  $SU(2)$  gaugino mass  $M_2$  we see the sharp change in the dilepton invariant spectra. Points (4 - 6) differ from CMS mSUGRA test point LM1 by both  $SU(2)$  gaugino mass and higgsino mass parameter  $\mu$ . For the points (7 - 10) the difference with point LM1 also includes the increase in gluino and LSP masses.

For the points (7 - 12) we have very sharp change in the number of dilepton events. For the luminosity  $\mathcal{L} = 1 \text{ fb}^{-1}$  after the cuts with  $p_T^{lept} > 20 \text{ GeV}$ ,  $E_T^{miss} > 300 \text{ GeV}$  the number of events without isolated leptons, with single isolated lepton and with two isolated leptons are presented in Table 5.

Table 5: The number of events with  $l = 0$ ,  $l = 1$ ,  $l = 2$  for background and points LM1, 1-12.

Point	$N(l = 0)$	$N(l = 1)$	$N(l = 2)$
Back.	20	524	652
LM1	2119	1278	166
1	1856	1950	430
2	1858	1104	187
3	1800	671	83
4	1910	1876	407
5	2002	513	34
6	1950	449	27
7	143	35	1
8	87	21	0
9	95	21	1
10	56	6	0
11	1587	11	1
12	1430	10	1

As it follows from Table 5 for points (7 - 12) the perspective to discover SUSY using the signature with single lepton or dileptons plus  $E_T^{miss}$  looks

hopeless. Moreover for the points (7 - 12) the use of more powerful from the SUSY discovery point of view signature *no leptons* + *jets* +  $E_T^{miss}$  also looks very problematic.

The invariant mass distributions of  $l^+l^-$  (solid line) and  $e^\pm\mu^\mp$  (dotted line) lepton pairs at the extensions of the point LM1 are shown in Figs.8-9. The distributions of 0 leptons, 1 lepton, 2 leptons and  $\geq 3$  leptons on  $E_T^{miss}$  for the modifications of the point LM1 are shown in Figs.10 - 13 for an integral luminosity  $\mathcal{L} = 1 \text{ fb}^{-1}$ . As one can see from Fig.10 for the points (7-10) there is sharp change in lepton spectra distributions on  $E_T^{miss}$  compared to the test point LM1, namely, the number of lepton events for the points (7 - 10) are much smaller than for the test point LM1. The same situation takes place for the  $E_T^{miss}$  spectrum of events without leptons, see Fig.11.

## 7 Conclusion

In this paper we studied the  $e^\pm\mu^\mp + E_T^{miss}$  and  $l^+l^- + E_T^{miss}$  signatures ( $l = e, \mu$ ) for different parameters  $\tan\beta$  of the MSSM model. With  $\tan\beta$  rising, we observed a characteristic change in the shape of dilepton mass spectra in  $l^+l^- + E_T^{miss}$  versus  $e^\pm\mu^\mp$  final states reflecting the decrease of  $\tilde{\chi}_2^0 \rightarrow l^+l^- \tilde{\chi}_1^0$  branching ratio. We also studied some non mSUGRA modifications of the point LM1. We have found the drastic change in dilepton spectra with the increase of gaugino masses. For the points (7 - 12) the perspective to discover SUSY using the signatures with leptons and  $E_T^{miss}$  looks hopeless. Even more powerful signature with *no leptons* + *jets* +  $E_T^{miss}$  looks rather pessimistic.

This work was supported by RFFI grant No 07-02-00256.

## References

- [1] As a recent review, see for example:  
N.V.Krasnikov and V.A.Matveev, Phys.Usp. **47** (2004) 643;  
hep-ph/0309200.
- [2] H.Baer, C.-H.Chen, F.Paige and X.Tata, Phys.Rev.D **50** (1994) 4508.
- [3] As a review, see for example:  
S.Abdullin *et al.*, CMS Note 1998/006.
- [4] D.Denegri, W.Majerotto and L.Rurua, Phys. Rev. **D60** (1999) 035008.
- [5] <http://cmsdoc.cern.ch/~abdullin/cmsjet.html>
- [6] N.V.Krasnikov, Mod.Phys.Lett. **A9** (1994) 791;  
N.V.Krasnikov, Phys.Lett.B **388** (1996) 783.
- [7] F.Deppisch *et al.*, hep-ph/0401243.
- [8] Reviews and original references can be found in:  
H.E.Haber and G.L.Kane, Phys. Rep. **117** (1985) 75;  
R.Barbieri, Riv.Nuovo.Cim. **11** (1988) 1;  
D.V.Nanopoulos, Phys.Rep. **145** (1987) 1;  
H.P.Nilles, Phys.Rep. **110** (1984) 1;  
N.V.Krasnikov and V.A.Matveev, Phys.Part.Nucl. **28** (1997) 441;  
N.Polonsky, Lect.NotesPhys. **M68** (2001) 1.
- [9] Yu.Andreev, S.Bitukov, N.Krasnikov and A.Toropin, CMS NOTE  
2006/103; hep-ph/0608176.
- [10] M.Chiorboli, M.Galanti and A.Tricomi, CMS NOTE 2006/133.
- [11] H.Baer, F.E.Paige, S.D.Protopopescu and X.Tata, hep-ph/0001086.
- [12] T.Sjostrand *et al.*, Comp.Phys.Comm. **135** (2001) 238;  
<http://www.thep.lu.se/~torbjorn/Pythia.html>
- [13] V.I.Savrin *et al.*, Nucl.Instr.Meth. **A534** (2004) 250.
- [14] W.Beenakker *et al.*, hep-ph/9611232;  
<http://people.web.psi.ch/spira/prospino/>

- [15] <http://cmsdoc.cern.ch/cmsoo/cmsoo.html>
- [16] [http://cmsdoc.cern.ch/cms/PRS/susybsm/msugra\\_testpts/msugra\\_testpts.html](http://cmsdoc.cern.ch/cms/PRS/susybsm/msugra_testpts/msugra_testpts.html)
- [17] M.Battaglia *et al.*, Eur.Phys.J. **C33** (2004) 273.
- [18] S.I.Bityukov and N.V.Krasnikov, Mod.Phys.Lett. **A13** (1998) 3235;  
S.I.Bityukov and N.V.Krasnikov, Nucl.Instr.Meth. **A452** (2000) 518.
- [19] V.Bartsch and G.Quast, CMS Note 2005/004;  
R.Cousins, J.Mumford and S.Valuev, CMS Note 2005/002.

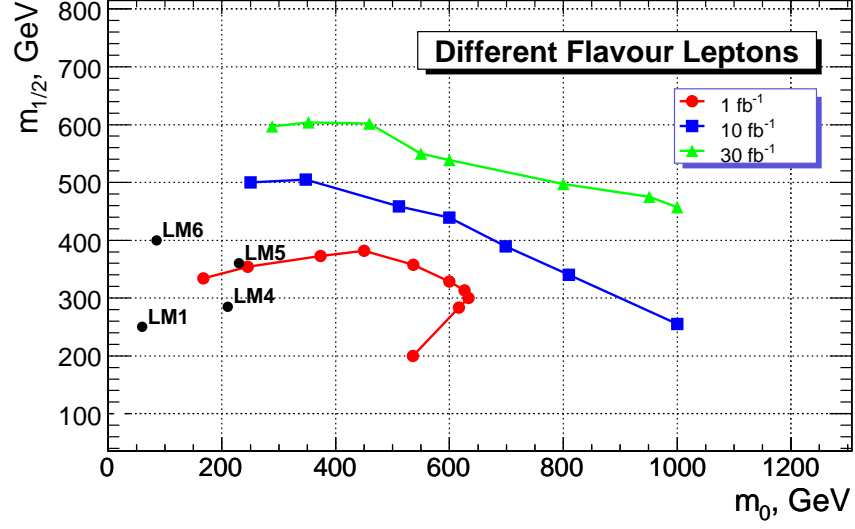


Figure 1:  $e^+\mu^- + e^-\mu^+$  discovery plot for  $\tan\beta = 10$ ,  $\text{sign}(\mu) = +$ ,  $A = 0$ . Two isolated leptons with  $p_T^{\text{lept}} > 20 \text{ GeV}/c$  and  $E_T^{\text{miss}} > 300 \text{ GeV}$  are selected.

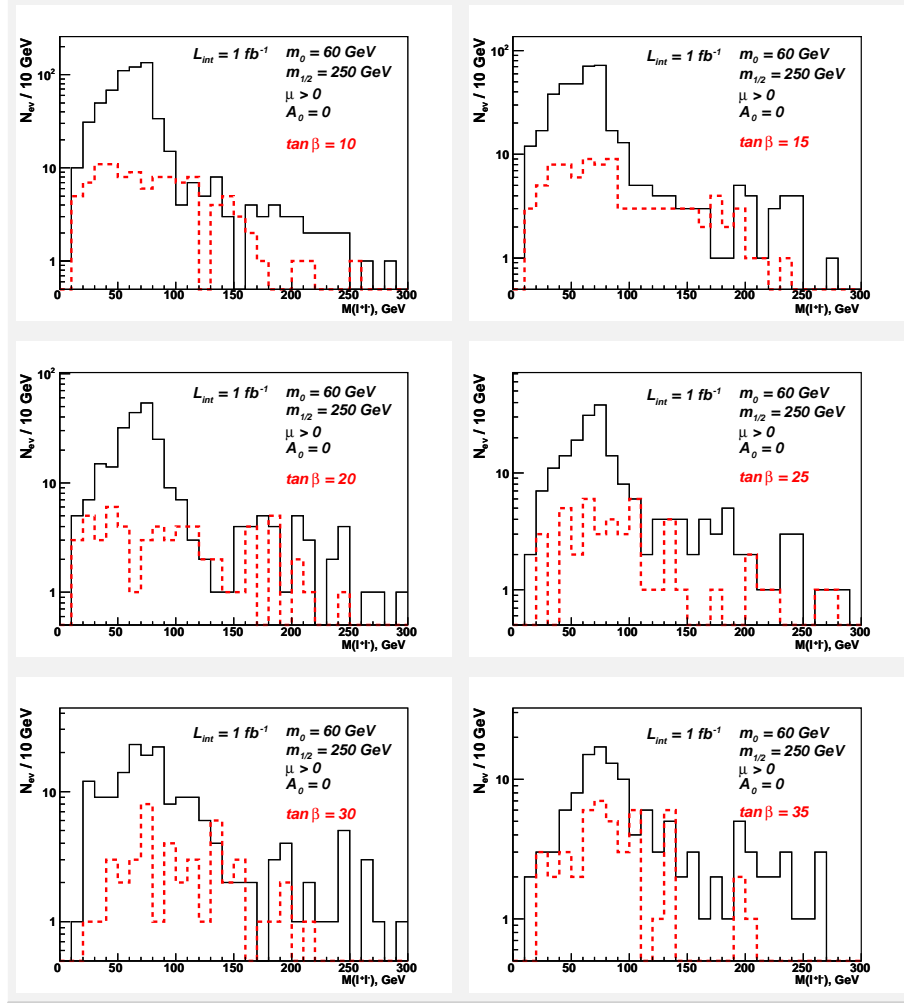


Figure 2: The invariant mass distributions of  $l^+l^-$  (solid line) and  $e^\pm\mu^\mp$  (dotted line) lepton pairs at the mSUGRA point  $m_0 = 60 \text{ GeV}$ ,  $M_{1/2} = 250 \text{ GeV}$ ,  $\mu > 0$ ,  $A = 0$  with various  $\tan\beta = 10, 15, 20, 25, 30, 35$ .

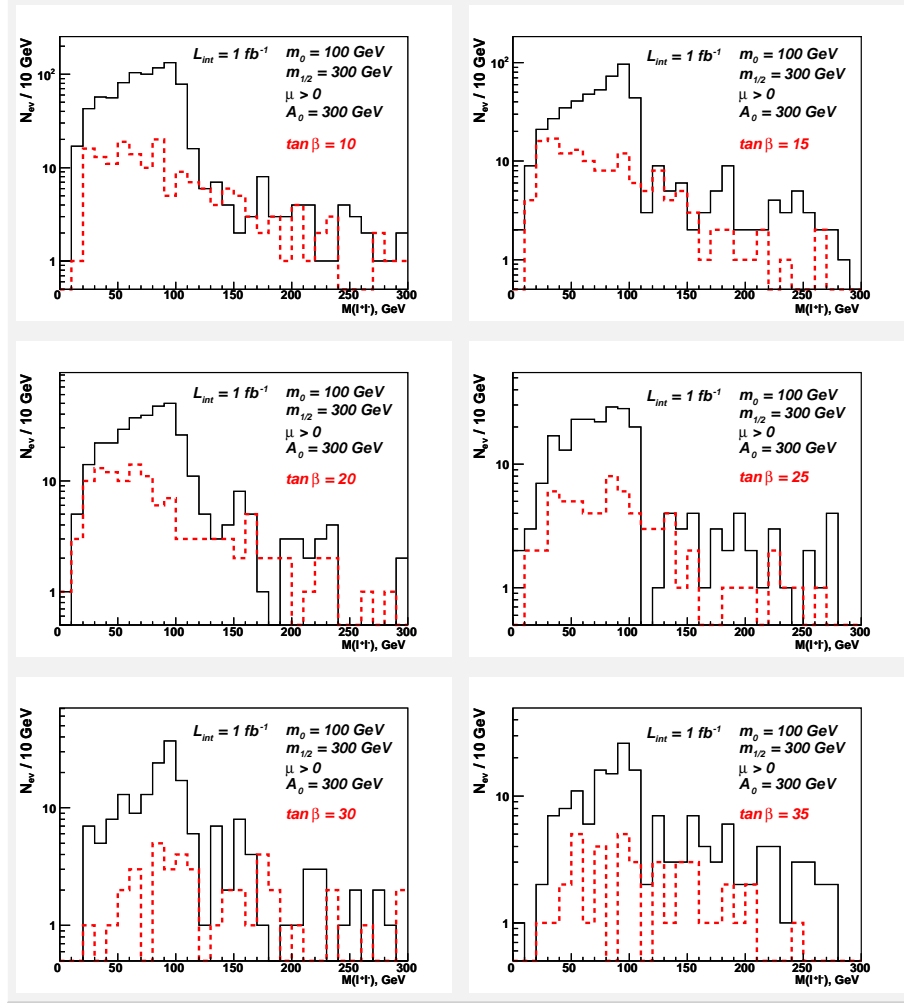


Figure 3: The invariant mass distributions of  $l^+l^-$  (solid line) and  $e^\pm\mu^\mp$  (dotted line) lepton pairs at the mSUGRA point  $m_0 = 100 \text{ GeV}$ ,  $M_{1/2} = 300 \text{ GeV}$ ,  $\mu > 0$ ,  $A = 300 \text{ GeV}$  with various  $\tan\beta = 10, 15, 20, 25, 30, 35$ .



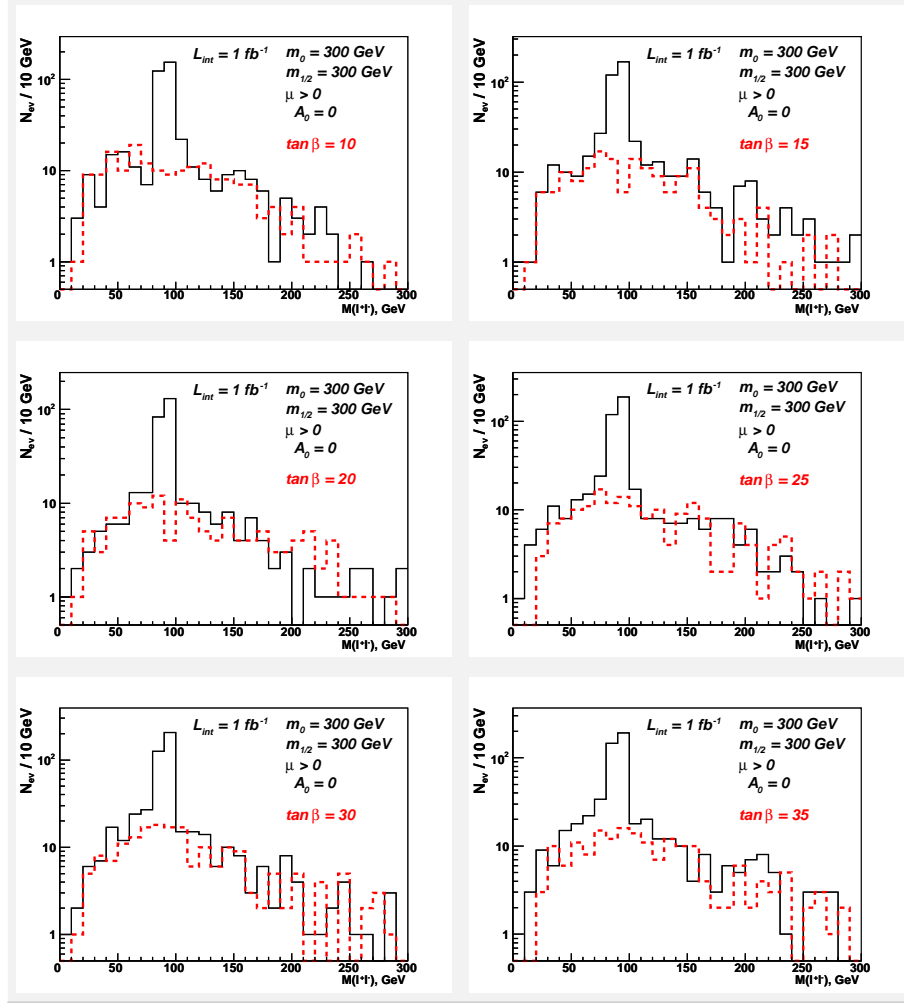


Figure 4: The invariant mass distributions of  $l^+l^-$  (solid line) and  $e^\pm\mu^\mp$  (dotted line) lepton pairs at the mSUGRA point  $m_0 = 300 \text{ GeV}$ ,  $M_{1/2} = 300 \text{ GeV}$ ,  $\mu > 0$ ,  $A = 0$  with various  $\tan\beta = 10, 15, 20, 25, 30, 35$ .

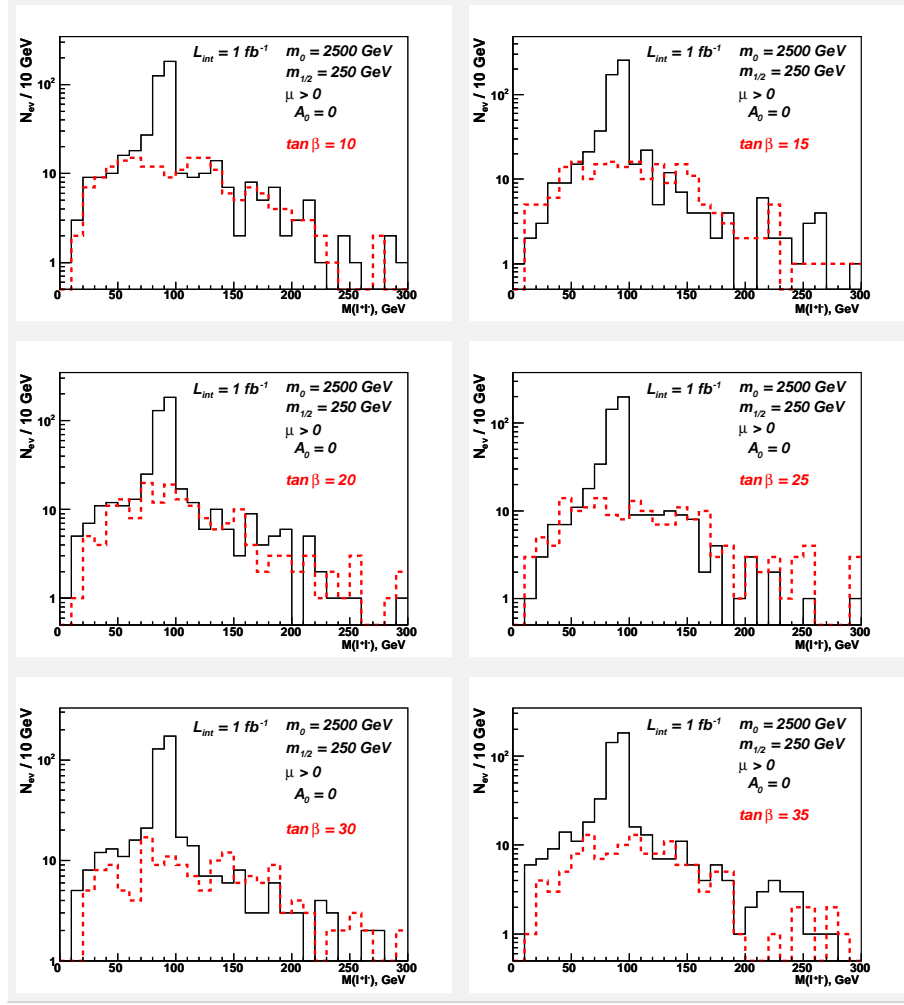


Figure 5: The invariant mass distributions of  $l^+l^-$  (solid line) and  $e^\pm\mu^\mp$  (dotted line) lepton pairs at the mSUGRA point  $m_0 = 2500 \text{ GeV}$ ,  $M_{1/2} = 250 \text{ GeV}$ ,  $\mu > 0$ ,  $A = 0$  with various  $\tan\beta = 10, 15, 20, 25, 30, 35$ .

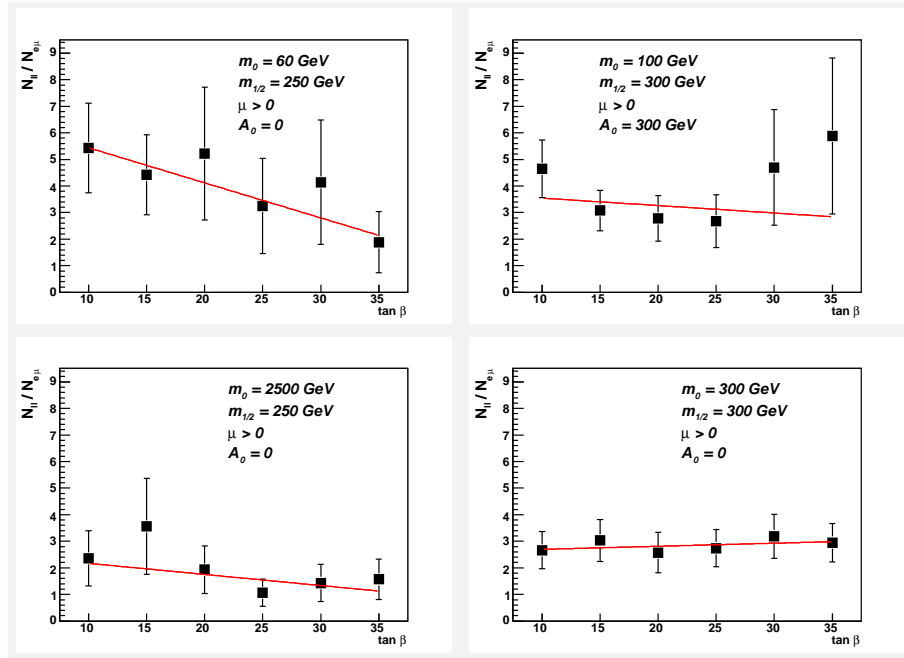


Figure 6: The dependence of the ratio  $N_S(l^+l^-)/N_S(e^\pm\mu^\mp)$  ( $N_S()$  is the number of events after the cuts  $p_T^{lept} > 20 \text{ GeV}$ ,  $E_T^{miss} > 300 \text{ GeV}$ ) on  $\tan \beta$  for different scenarios. Here the error is due to finite number of simulated events.

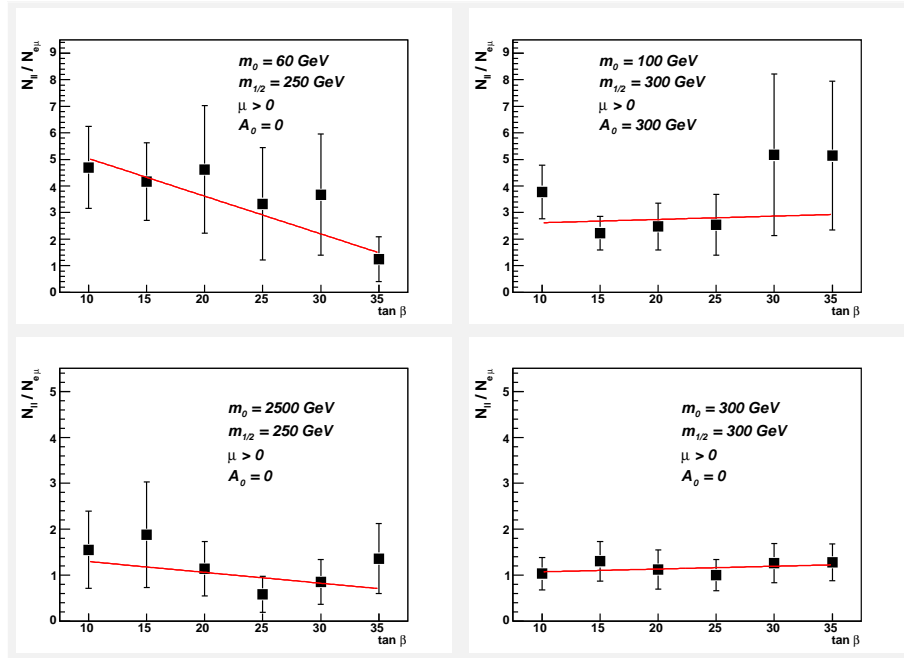


Figure 7: The dependence of the ratio  $N_S(l^+l^-)/N_S(e^\pm\mu^\mp)$  ( $N_S()$  is the number of events after the cuts  $p_T^{lept} > 20 \text{ GeV}$ ,  $E_T^{miss} > 300 \text{ GeV}$ ,  $|M_{inv} - M_Z| > 15 \text{ GeV}$ ), on  $\tan \beta$  for different scenarios. Here the error is due to finite number of simulated events.

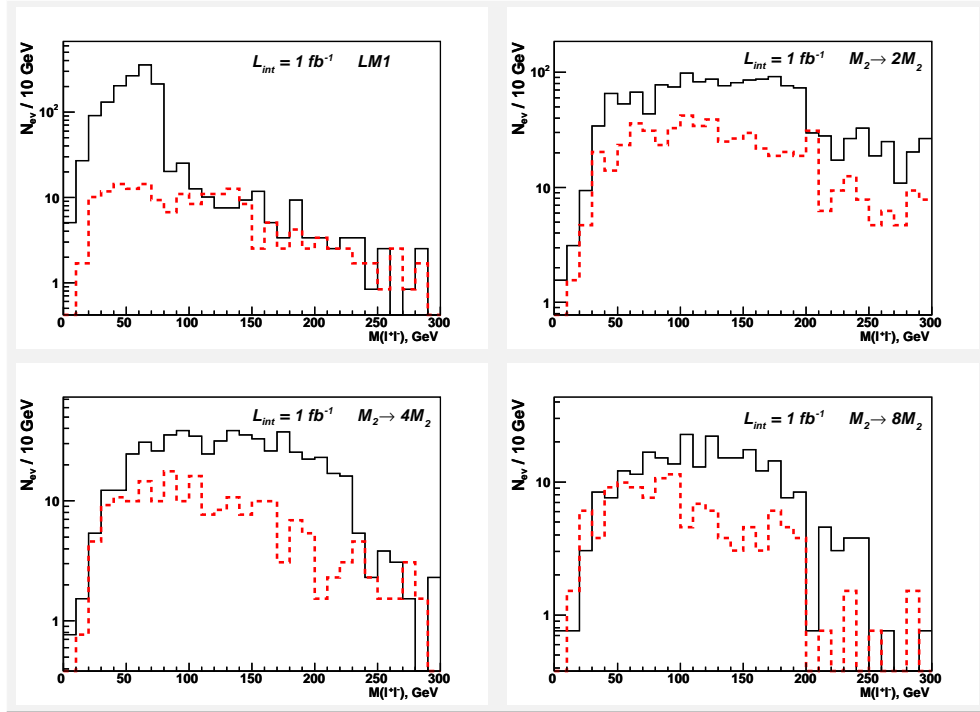


Figure 8: The invariant mass distributions of  $l^+l^-$  (solid line) and  $e^\pm\mu^\mp$  (dotted line) lepton pairs at the extensions of the point LM1.

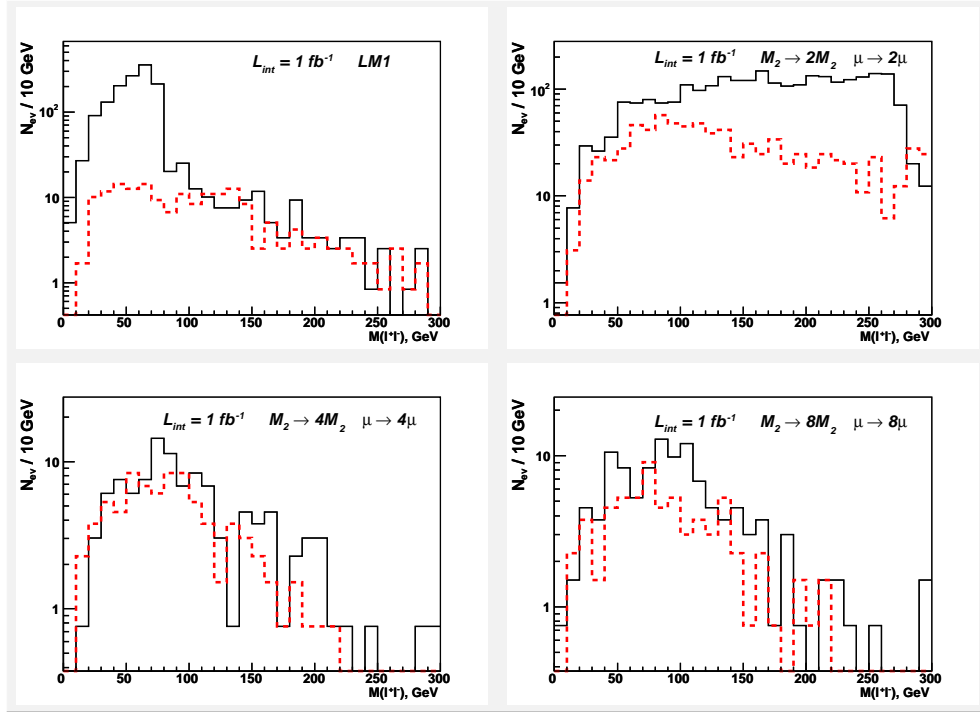


Figure 9: The invariant mass distributions of  $l^+l^-$  (solid line) and  $e^{\pm}\mu^{\mp}$  (dotted line) lepton pairs at the extensions of the point LM1.

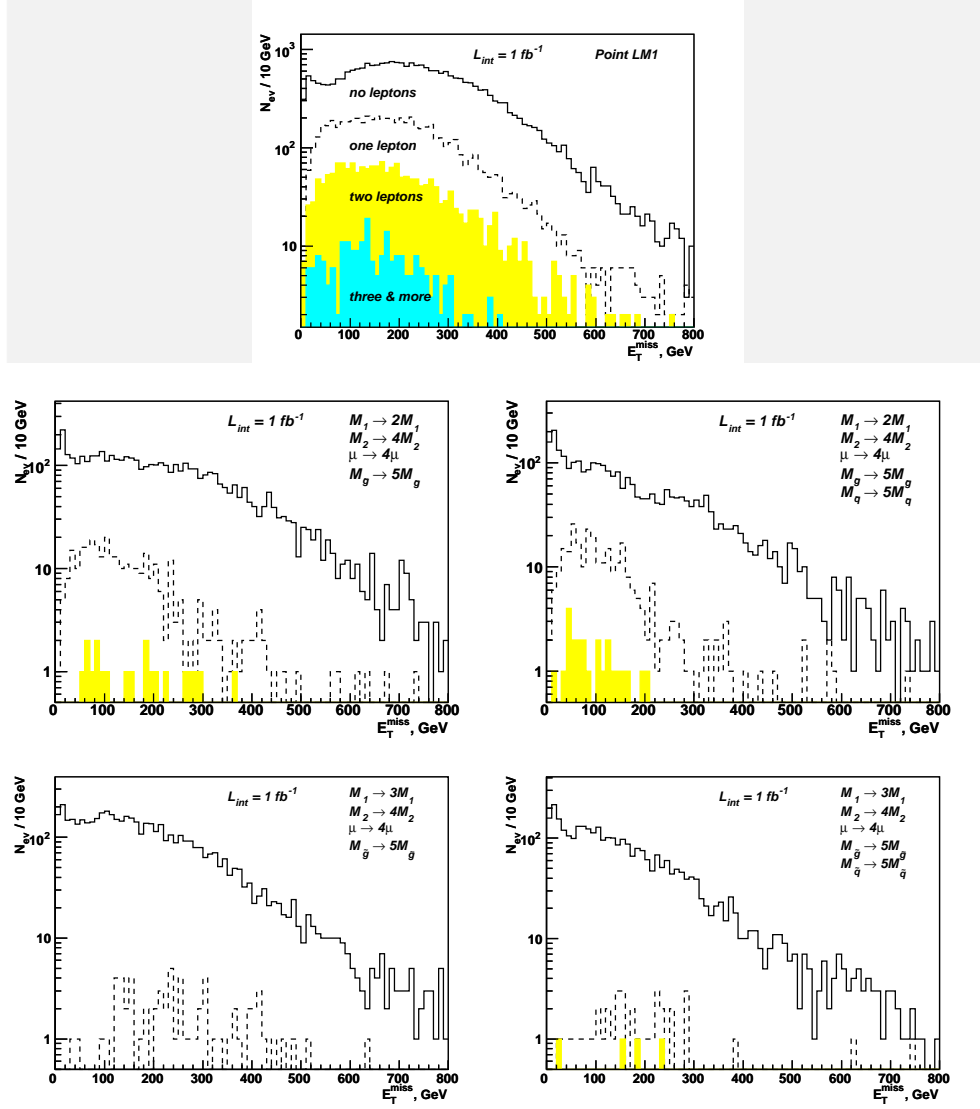


Figure 10: The  $E_T^{miss*}$  distributions for different modifications of the point LM1.

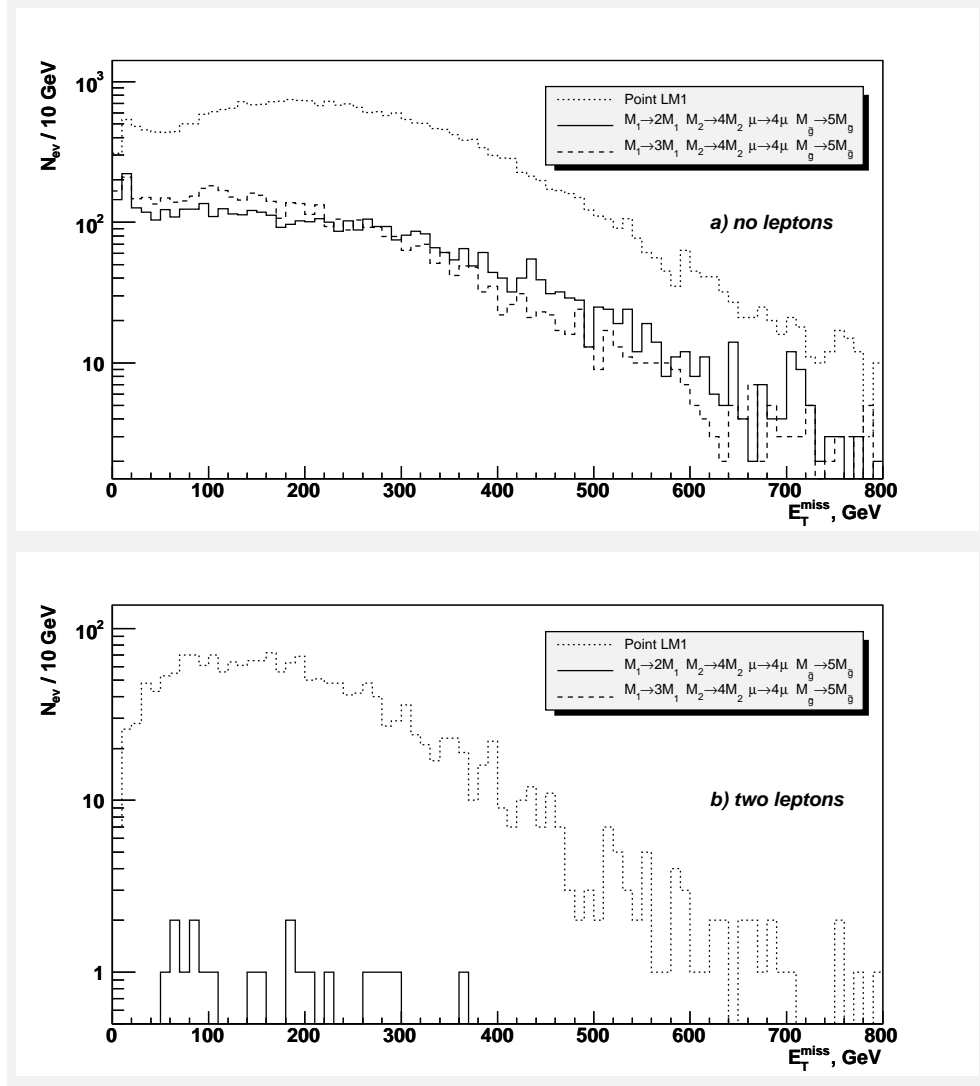


Figure 11: The  $E_T^{miss}$  distributions for the points LM1, 7 and 8 for the cases of no leptons and two leptons with  $p_T^{lept} > 20 \text{ GeV}$ .



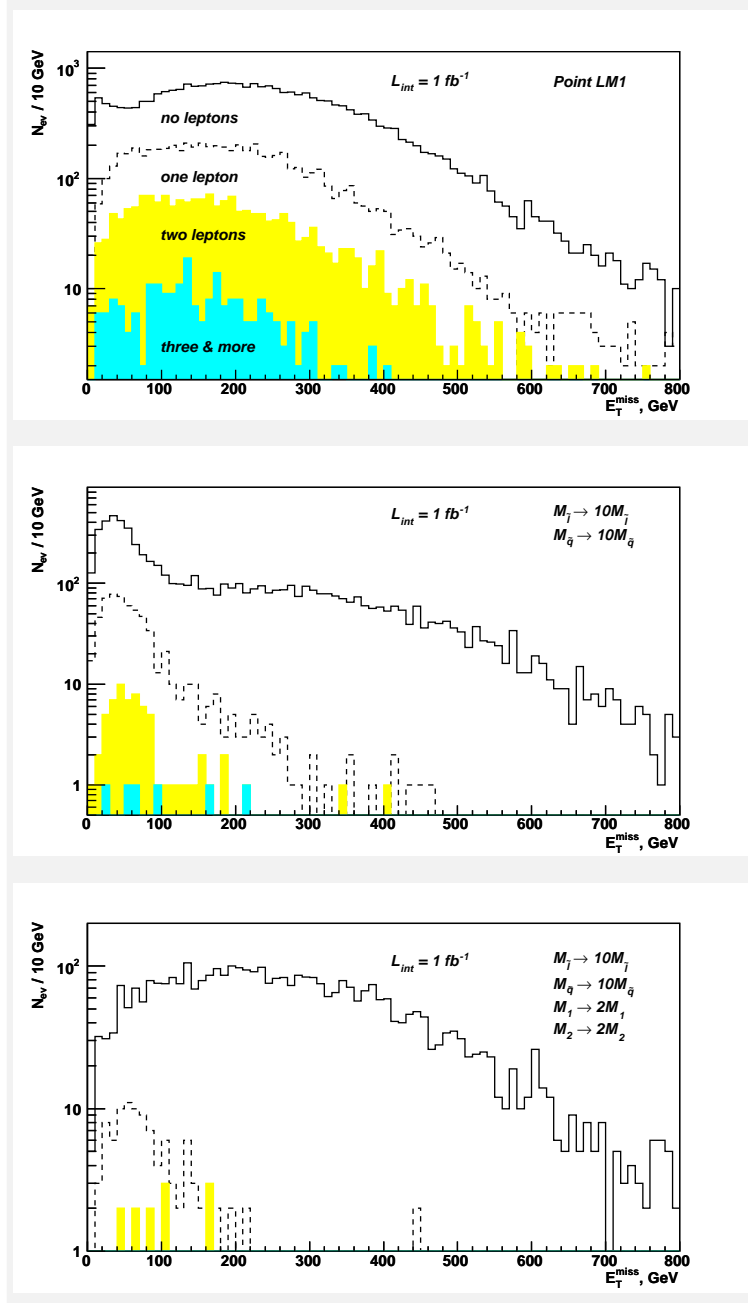


Figure 12: The  $E_T^{\text{miss}}$  distributions for the points LM1, 11 and 12.

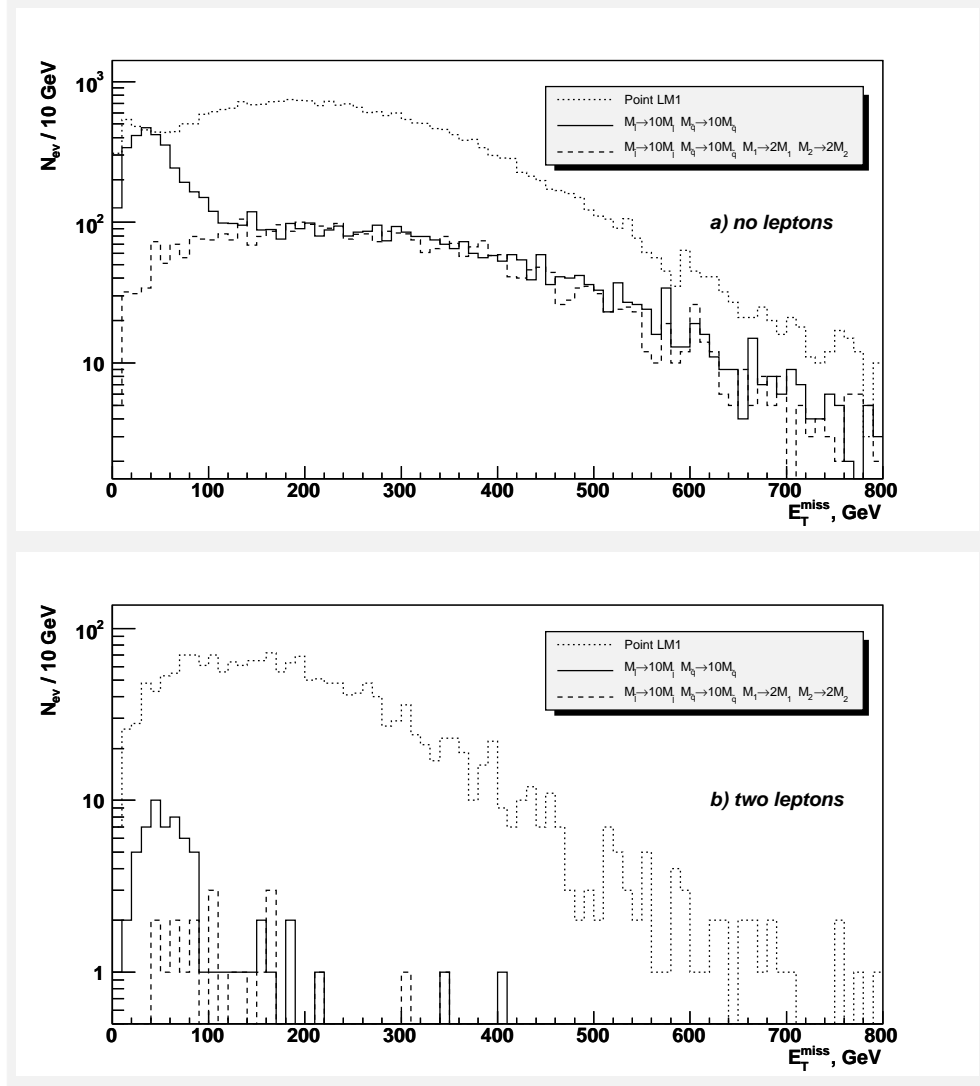


Figure 13: The  $E_T^{miss}$  distributions for points LM1, 11 and 12 for the cases of no leptons and two leptons with  $p_T^{lept} > 20 \text{ GeV}$ .